American Mineralogist, Volume 61, pages 435–447, 1976

High-temperature structural study of the $P2_1/a \rightleftarrows A2/a$ phase transition in synthetic titanite, $CaTiSiO_5$

MARK TAYLOR AND GORDON E. BROWN

Department of Geology, Stanford University
Stanford, California 94305

Abstract

Synthetic $CaTiSiO_5$ has been shown to undergo a reversible, displacive phase transition at 220° ± 20°C from space group $P2_1/a$ to $A2/a$, using high-temperature single crystal X-ray diffraction techniques. The transition is signaled by disappearance of reflections of the type hkl: $k + l$ odd. The structure of a synthetic $P2_1/a$ sphene has been refined at 25°C, 165°C, 270°C, 515°C, and 740°C to conventional R-factors of 0.048, 0.047, 0.033, 0.039, and 0.043, respectively. The principal structural change characterizing the phase transition involves a movement of the titanium atom from a position displaced toward one corner of the TiO_6 octahedron to a position at the geometric center of the octahedron, a shift of 0.10 Å. Ti–O bonds to the corner-shared oxygens change from 1.77 and 1.97 Å at room temperature to 1.87 Å at 270°C. Above the transition further atomic movement is slight and is consistent with simple cell expansion. The transition mechanism is similar to other displacive transitions in silicates and perovskite structure ferroelectrics and may lead to domain formation.

Introduction

Titanite (sphene) is an accessory mineral common to a wide variety of lithic environments. When euhedral crystals occur with characteristic sphenoidal cross-section or as dove-tailed twin intergrowths, it is one of the most easily recognized accessory minerals in igneous rocks. Although the structure of titanite was determined initially by Zachariasen (1930) and refined more recently by Mongiore and Riva de Sanseverino (1968), new observations of weak reflections violating the assigned space group symmetry $A2/a$ in a synthetic titanite (Robbins, 1968) led Speer and Gibbs (1974) to reanalyze the structure in space group $P2_1/a$. They also observed these weak primitive reflections (hkl: $k + l = 2n + 1$) in several natural titanites. Differences in the diffuseness of these $k + l$ odd reflections among the synthetic and natural specimens led them to suggest that natural titanites possess a domain structure consisting of $P2_1/a$ domains related by a half-turn parallel to b.

Because of apparent similarities between these observations and those for pigeonites and primitive cummingtonites, which undergo non-quenchable, reversible phase transitions from primitive to end-centered unit cells at elevated temperatures, we undertook the present high-temperature X-ray study of a synthetic titanite showing weak primitive reflections. The results of this study including the discovery of a reversible, non-quenchable phase transition from $P2_1/a$ to $A2/a$ symmetry are reported below. A preliminary account of this study was reported earlier by Taylor and Brown (1974).

Experimental details

Crystals of synthetic $CaTiSiO_5$ grown from an homogeneous glass at 1200°C were kindly provided by Professor G. V. Gibbs from the same sample used by Speer and Gibbs (1974); the reader is referred to their paper (Speer and Gibbs, 1976) for details of the synthesis. A qualitative spectral scan on an electron microprobe showed only trace amounts (<0.5%) of aluminum as a contaminant. A clear fragment measuring 0.07 × 0.15 × 0.15 mm was mounted for examination on a precession camera. After preliminary alignment and X-ray examination, the crystal was remounted in high-temperature mullite cement and sealed in an evacuated silica glass capillary. The c^* axis was oriented parallel to the rotation axis of the goniometer head.

The search for a phase transition was initiated with precession photographs of the $h0l$ net at a number of temperatures to 300°C. The $h0l$ net was chosen be-

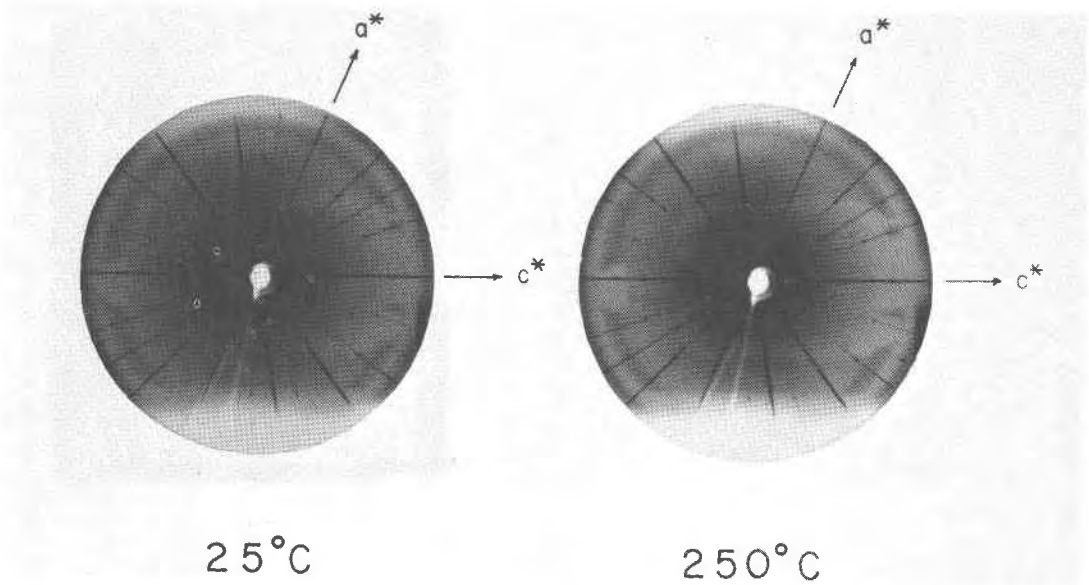

FIG. 1. *h0l* precession photographs of synthetic titanite (unfiltered Mo*K* radiation, 36 kV, 16 mA, 48 hour exposure) taken at 24°C (1a) and 250°C (1b). The weak violations of *A*2/*a* symmetry (*hkl*: $k + l \neq 2n$) are clearly visible along the zone 40*l* in 1a.

cause it shows the strongest violations of *A*2/*a* symmetry. A Supper precession camera equipped with the heating attachment described by Brown *et al.* (1973) was used in these experiments. Figure 1 shows *h0l* precession photographs taken at room temperature (1a) and 250°C (1b). Unfiltered, long exposure (up to 100 hrs.) photographs at 250°C showed no violations of the *A*2/*a* symmetry whereas short exposures (24 hrs) at 150°C showed them quite clearly. No broadening or weakening of the violating reflections was observed after repeated heatings and coolings over a 3 week period.

After bracketing the transition temperature between 200 and 250°C, the crystal was transferred to a Picker FACS-I diffractometer equipped with a chi-circle heating attachment (Brown *et al.*, 1973). The heater was calibrated by observing the melting of crystals mounted in the same fashion and in the same position as the crystal used in the high-temperature diffraction experiment. The melting points of benzoic acid (123°C), d-camphoric acid (187°C), anthracene (216°C), sodium nitrate (306.8°C), barium nitrate (592°C), potassium chloride (776°C), sodium chloride (801°C), and barium chloride (962°C) were used for calibration. While the furnace has an apparent stability of approximately ±10°C, problems with calibration place an uncertainty of ±20°C on all reported temperatures.

The phase transition was next examined by monitoring the intensity of the $\bar{4}01$ reflection as a function of temperature. After alignment at 165°C, the $\bar{4}01$ reflection was automatically centered, and all slits were opened so that slight misalignments during subsequent heating would have little effect on the observed intensity. Thirty-second intensity measurements at peak maximum were made as the crystal was heated at a rate of ~1°C/minute from 165°C to 300°C. The results of this experiment are shown in Figure 2. The crystal was then allowed to cool through the transition as the intensity was monitored. No hysteresis was detected, and the intensity of the $\bar{4}01$ returned to the level observed before heating. Crude temperature jump experiments showed that the transition has no apparent time dependence within the response time of the heater. The transition temperature of 220° ± 20°C was confirmed by 2θ scans through several additional strong primitive reflections ($\bar{4}03$, $\bar{8}03$) at a number of temperatures.

Intensity data were gathered at 25°, 165°, 270°, 515°, 740°, and then again at 25°C. The crystal was allowed to equilibrate for 24 hours and realigned at each temperature before data collection. Cell parameters at each temperature were obtained by least-squares refinement using the angular settings of twelve automatically centered reflections (>30°2θ). These results are listed in Table 1. The apparent shortening of the *a* cell edge at 270°C was confirmed by centering a second set of twelve reflections. In each

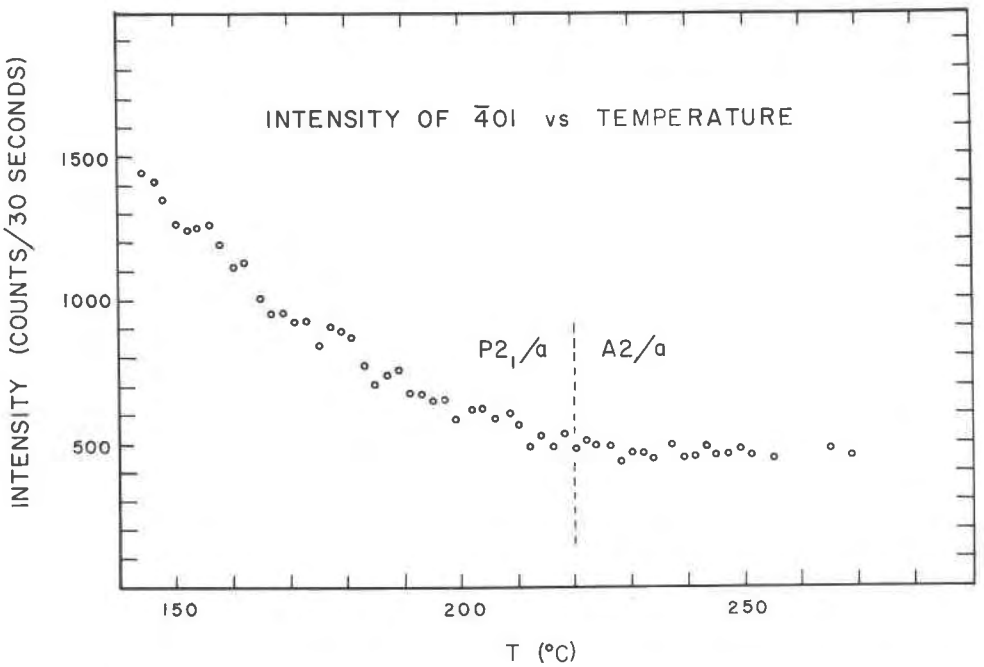

FIG. 2. Intensity versus temperature for the $\bar{4}01$ reflection. The dashed vertical line is drawn at the estimated transition temperature (220° ± 20°C). Off-peak background counts are approximately 500 counts/30 seconds corresponding to the intensity of $\bar{4}01$ above 220°C.

case graphite monochromatized Mo$K\alpha$ radiation (36 kV, 16 mA) was used with the tube set at a take-off angle of 2.5°. Approximately 650 reflections within the 2θ range 5° to 50° were collected at each temperature using the θ–2θ scan technique at a scan rate of 1°/minute and a scan range of 2.5° plus the α_1–α_2 dispersion. Background radiation was recorded for 10 seconds at the high and low angle ends of each scan. Two standard reflections (004, 060) were measured every 30 reflections as a check of crystal alignment as well as electronic fluctuations, both of which proved to be negligible over the course of the experiment. During data collection at 165°, 270°, 515°, and 740°C, crystal temperature was recorded continuously by means of a strip chart recorder and varied less than ±10°C in each case.

The intensity data were corrected for Lorentz and polarization effects, assuming a fifty percent ideally mosaic monochromator crystal. Because of the small size and low absorption coefficient of the crystal (μ =

TABLE 1. Cell parameters of synthetic titanites at five temperatures

Temperature (°C)	a(Å)	b(Å)	c(Å)	β(°)	V(Å^3)
25	7.068(1)*	8.714(3)	6.562(2)	113.82	369.7
165	7.067(1)	8.726(2)	6.568(2)	113.77	370.7
270	7.060(2)	8.737(3)	6.565(3)	113.73	370.7
515	7.077(2)	8.743(4)	6.584(3)	113.68	373.1
740	7.083(4)	8.753(9)	6.596(7)	113.55	374.8
%Δ**	0.21	0.45	0.50	0.24	1.38

*Numbers in parentheses represent the estimated standard error ($1\hat{\sigma}$) in the last decimal place.

**% change between 25 °C and 740°C.

39.38 cm^{-1}; $\mu R = 0.23$), no absorption correction was applied. Standard deviations were estimated using the formula suggested by Corfield *et al.* (1967) with a diffractometer factor of 0.04. Refinement of the 25° and 165°C structures was initiated in space group $P2_1/a$ using coordinates derived from those of Mongiorgi and Riva de Sanseverino (1968). We shifted the origin of their $A2/a$ structure by 1/4 y and 1/4 z to facilitate comparison of the low temperature $P2_1/a$ and high temperature $A2/a$ structures. Reflections with $F^2 < 3\sigma(F^2)$ were considered unobserved and were not used in the refinement. Very strong reflections for which calculated and observed structure factors differed by more than 15.0 were not included in the refinement, though only 1 to 3 of these were found in each data set. Seven cycles of isotropic refinement with unit weights and four cycles of full anistropic refinement with weights based on counting statistics were computed using L. W. Finger's RFINE program. Unionized atomic scattering factors from Doyle and Turner (1968), anomalous dispersion corrections from Vol. III of International Tables, and a secondary extinction correction were applied.

Neither of the refinements described above converged properly. Furthermore Ca and Ti showed displacements along the c axis which were felt to be inconsistent with the diffraction pattern. The lack of reflections violating $A2/a$ symmetry in the 25°C and 165°C $0kl$ zone suggested that the atomic displacement producing $P2_1/a$ symmetry is primarily along the a direction. With this possibility in mind, a new set of least-squares cycles was run, starting with the atomic parameters of Mongiorgi and Riva de Sanseverino (1968), but constraining Ca, Ti, Si, and O(1) to movement only in the x direction. Four such cycles of isotropic refinement followed by additional cycles of isotropic and anisotropic refinement, during which all atomic parameters, a scale factor, and a secondary extinction parameter were allowed to vary, led to convergence and final unweighted (weighted) R-factors of 0.048 (0.063) and 0.047(0.059) for the 25°C and 165°C structures, respectively. Those pairs of atoms [O(2A), O(2B), O(3A) and O(3B)] approaching crystallographic equivalence as the transition is approached showed high correlation coefficients with respect to positional parameters. For example, the correlation coefficient for the x coordinates of O(2A) and O(2B) at 165°C is 0.80. These high correlations may have caused the anisotropic temperature factors of several atoms in both data sets to be non-positive definite [25°C: O(1), O(2B);165°C: O(1), O(2A), O(2B), O(3A)].

Refinement of the high-temperature ($A2/a$) titanite structure at 270°, 515°, and 740°C was carried out in the same manner as previously described and converged after four isotropic and five anistropic cycles of least squares. None of the problems encountered in the refinements of the 25°C and 165°C data sets were found in these refinements of the $A2/a$ structure. Details of the five refinements are given in Table 2. Table 3 contains listings of the observed and calcu-

TABLE 2. Refinement parameters for synthetic titanite at five temperatures

Parameter	25°C	165°C	270°C	515°C	740°C
No. Least-Squares Variables	74	74	41	41	41
No. Reflections*	430	355	276	256	267
R**	0.048	0.047	0.033	0.039	0.043
R(weighted)***	0.063	0.059	0.044	0.049	0.054
$\hat{\sigma}$(unit weight observation)	2.00	1.94	1.59	1.71	1.84
Maximum correlation coefficient****	0.63	-0.84	0.55	0.57	0.56

Included in final cycle of refinement. Reflections with $F^2 < 3\sigma(F^2)$ or with $|F_o - F_c| > 15$ were rejected. There were only 1 to 3 satisfying the latter condition in each refinement.

$R = \Sigma\,(|F_o| - |F_c|)/\Sigma|F_o|$ *$R(wt.) = [\Sigma w(|F_o| - |F_c|)^2/\Sigma wF_o^2]^{\frac{1}{2}}$

****Among atomic parameters.*

TABLE 4. Refined positional and isotropic thermal parameters for synthetic titanite at five temperatures

Atom	Parameter	25°C	165°C	270°C	515°C	740°C
Ca	x	0.2439(6)**	0.2434(11)	0.25	0.25	0.25
	y	0.4184(2)	0.4185(2)	0.4187(2)	0.4187(2)	0.4191(2)
	z	0.2513(8)	0.2521(16)	0.25	0.25	0.25
	B(eq)***	1.26(5)	1.56(6)	1.81(4)	2.41(6)	2.94(6)
Ti	x	0.5124(2)	0.5110(4)	0.50	0.50	0.50
	y	0.2557(4)	0.2528(10)	0.25	0.25	0.25
	z	0.7498(4)	0.7504(8)	0.75	0.75	0.75
	B(eq)	0.60(4)	0.82(5)	1.05(4)	1.26(4)	1.47(5)
Si	x	0.7494(7)	0.7536(11)	0.75	0.75	0.75
	y	0.4327(2)	0.4328(3)	0.4331(2)	0.4330(3)	0.4328(3)
	z	0.2493(9)	0.2492(21)	0.25	0.25	0.25
	B(eq)	0.40(5)	0.52(5)	0.62(4)	0.76(6)	0.93(6)
O(1)	x	0.7497(10)	0.7519(16)	0.75	0.75	0.75
	y	0.3212(6)	0.3206(8)	0.3197(6)	0.3212(8)	0.3210(8)
	z	0.7498(15)	0.7513(26)	0.75	0.75	0.75
	B(eq)	0.70(10)	0.90(13)	1.06(10)	1.38(13)	1.70(13)
O(2A)	x	0.9095(9)	0.9110(16)	0.9104(5)	0.9102(7)	0.9093(7)
	y	0.3175(8)	0.3186(11)	0.3160(4)	0.3166(5)	0.3167(5)
	z	0.4329(13)	0.4365(22)	0.4342(6)	0.4346(7)	0.4341(8)
	B(eq)	0.75(15)	0.90(26)	1.05(7)	1.37(9)	1.73(10)
O(2B)	x	0.0870(9)	0.0901(18)	———	———	———
	y	0.1851(8)	0.1861(13)	———	———	———
	z	0.0626(12)	0.0660(20)	———	———	———
	B(eq)	0.60(14)	0.96(24)	———	———	———
O(3A)	x	0.3813(10)	0.3813(15)	0.3820(5)	0.3816(6)	0.3817(6)
	y	0.4586(9)	0.4582(14)	0.4600(4)	0.4603(6)	0.4601(6)
	z	0.6448(13)	0.6442(23)	0.6467(6)	0.6477(7)	0.6482(8)
	B(eq)	0.52(14)	0.82(28)	1.00(7)	1.29(9)	1.57(10)
O(3B)	x	0.6178(10)	0.6179(16)	———	———	———
	y	0.0381(9)	0.0384(13)	———	———	———
	z	0.8520(13)	0.8504(23)	———	———	———
	B(eq)	0.73(15)	0.95(29)	———	———	———

Parameters from final cycle of anisotropic refinement.

**Numbers in parentheses represent the estimated standard error ($1\hat{\sigma}$) in the last decimal place quoted.*

***Equivalent isotropic temperature factors were calculated using the expression of Hamilton (1959).*

lated structure factors from the final cycles of refinement of the 25°C and 270°C data sets.[1] The final positional and isotropic equivalent thermal parameters are listed in Table 4.

Results and discussion

Comparison of low- and high-temperature titanite structures

The primary structural unit of titanite in both the low-temperature ($P2_1/a$) and high-temperature ($A2/a$) modifications consists of a zig-zag chain of corner-sharing TiO_6 octahedra running parallel to the a axis as shown in Figure 3a. Isolated SiO_4 tetrahedra share corners with these octahedra and serve as intra- and inter-chain links through the O(2) and O(3) oxygens, respectively. The intra-chain linkage is strikingly similar to that of the 7 Å, corner-linked octahedral chain of the phosphate laueite (Moore, 1970). Ca occupies an irregular seven-coordinated site between the octahedral chains (Figure 3a). The four O(1) anions in each unit cell are three-coordinated by two Ti and one Ca. Each of the eight O(2) anions is three-coordinated by Si, Ti, and Ca. The eight O(3) anions per unit cell are four-coordinated by Si, Ti, and two Ca cations. Additional details of the low-temperature structure can be found in Speer and Gibbs (1976).

[1] Table 3 may be obtained by requesting document AM-76-014 from the Business Office, Mineralogical Society of America, Suite 1000, lower level, 1909 K Street, N.W., Washington, D.C. 20006. Please remit $1.00 in advance for the microfiche.

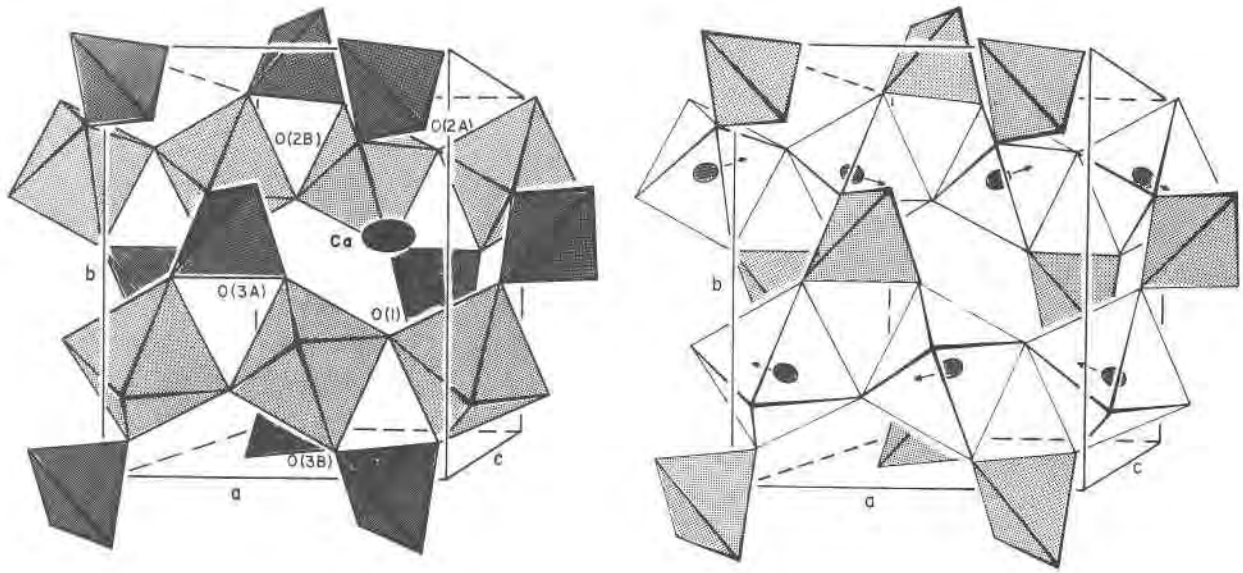

FIG. 3. (a) Perspective drawing of the titanite structure projected on (001) showing the zig-zag chain of Ti-octahedra crosslinked by isolated Si-tetrahedra. One of the Ca-cations is shown in its seven-coordinated site between the chains. The five nonequivalent oxygens in space group $P2_1/a$ are labeled following the notation used in Tables 4 and 5. (b) Perspective drawing of the titanite structure projected on (001) showing the direction of movement of Ti-cations accompanying the phase transition.

In order to facilitate comparison between the $P2_1/a$ and $A2/a$ titanite structures we represent their coordination formulae below following the recently introduced notation of Muller and Roy (1974).

$P2_1/a$ *titanite structural formula*

$$Ca^{VII}Ti^{VI}Si^{IV}O_3{}^{III}O_2{}^{IV}$$

$$\{Ca^{7\times I}_{[1]}\ Ti^{6\times I}_{[1]}\ Si^{4\times I}_{[1]}\ O(1)^{I+I+I}_{[1]}\ O(2A)^{(I)+I+I}_{[1]}\ O(2B)^{(I)+I+I}_{[1]}\ O(3A)^{(I)+I+I+I}_{[1]}\ O(3)B^{(I)+I+I+I}_{[1]}\}$$

$A2/a$ *titanite structural formula*

$$Ca^{VII}Ti^{VI}Si^{IV}O_3{}^{III}O_2{}^{IV}$$

$$\{Ca^{I+II+II+II}_{[2]}\ Ti^{II+II+II}_{[\bar{1}]}\ Si^{II+II}_{[2]}\ O(1)^{II+I}_{[2]}\ O(2)_2{}^{(I)+I+I}_{[1]}\ O(3)_2{}^{(I)+I+I+I}_{[1]}\}$$

The conventional structural formula is given above each Muller-Roy formula with the Roman numeral superscripts referring to coordination number. It should be noted that the phase transition does not involve a change in cation or anion coordination number. The subscripts in square brackets of the Muller-Roy formulae refer to the site symmetry of the atom position in Hermann-Mauguin notation; the superscripts refer to the number of equivalent and non-equivalent oxygen anions. The Ca cation in the $A2/a$ structure resides on a special position with site symmetry *2* and is coordinated by three different sets of two equivalent oxygen anions and a seventh non-equivalent oxygen. The parentheses around the first Roman numeral superscript of the O(2) and O(3) oxygen anions indicate that the nearest neighbor is a Si cation. Further explanation of the symbolism can be found in Muller and Roy (1974).

In the low-temperature $P2_1/a$ modification of titanite, all atoms occupy general positions of site symmetry *1*. The distinguishing feature of the low-temperature structure is the displacement of Ti toward the O(1) oxygen (see Fig. 3b). Although the equatorial oxygens, O(2A), O(2B), O(3A) and O(3B), have bonds to Ti about equal to the sum of the ionic radii (2.00 Å), the average Ti–O(1) bond length is 1.87 Å. The Ti-octahedron is therefore contracted in the axial direction [parallel to O(1)–Ti–O(1′)]. In spite of this contraction, Ti is displaced by 0.10 Å toward one of the O(1) oxygens resulting in Ti–O(1) bond lengths of 1.768 and 1.970 Å at 25°C. These distances are in good agreement with those reported by Speer and Gibbs (1974). The structure at 165°C shows the same general features as at 25°C; thermal parameters are higher and Ti is closer to the geometric center of its octahedron.

The most significant change in the structure as a function of temperature up to the transition is the movement of Ti from a general position off-set from

TABLE 5. Displacements (in Å) Between low (25°C) and high (270°C) titanite atom positions

Displacement (Å)	Ca	Ti	Si	O(1)	O(2A)	O(2B)	O(3A)	O(3B)
Parallel to a	0.043	-0.088	0.004	0.002	0.006	-0.018	0.005	0.001
Parallel to b	0.003	-0.050	0.003	-0.013	-0.013	-0.010	0.012	0.017
Parallel to c	-0.048	0.001	0.005	0.001	0.009	0.017	0.012	0.009

the center of the octahedron in the low-temperature form (site symmetry *1*) to the geometric center of the octahedron (site symmetry $\bar{1}$) in the high-temperature form. The displacement vectors associated with each Ti are shown exaggerated in Figure 3b, and the shifts in positional parameters over the temperature range 25° to 270°C are listed in Table 5. The shift in Ti position is primarily along *a* (Δx = 0.088 Å). The question must now be asked whether the Ti atom position in the high-temperature structure represents an average of two or more Ti positions or a single Ti position with a large thermal component in the axial direction of the octahedron. The major axis of the Ti thermal ellipsoid is aligned parallel to the O(1)–Ti–O(1) bond with an RMS displacement of 0.137 Å at 270°C. This displacement is somewhat larger than that of Ti from the geometric center of the octahedron in the low-temperature form, suggesting that the high-temperature form may represent a statistical average of two sites on either side of the center of symmetry. We feel, however, that such a situation would require a larger, more elongate ellipsoid. The evidence available is not clear cut, but in future discussion we will assume a single Ti site at the geometric center of the octahedron above 220°C. The only other atom that undergoes significant movement near the phase transition is Ca with shifts along *x* and *z* of 0.043 Å and −0.048 Å, respectively. Further shifts in positional parameters not fixed by symmetry are minor over the temperature range 270° to 740°C. Selected bond distances and angles at the various temperatures are given in Tables 7 and 8, respectively.

Polyhedral distortions and volume changes

Angular distortions were evaluated using the bond angle variance parameter of Robinson *et al.* (1971) (Table 9). The SiO_4 variance parameter reflects significant distortions from ideal tetrahedral angles and changes insignificantly with increasing temperature. The bond angle variance for the TiO_6 octahedron drops sharply at the transition, but this change reflects the movement of the Ti atom rather than any real change in the oxygen environment around the Ti site. With the exception of the Ti–O(1) bond, Ti–O and Ca–O bond lengths increase at roughly constant rates over the temperature range studied. Si–O bonds increase slightly but erratically with increasing temperature. The Si–O(3A) bond length at 165°C (1.685) seems anomalously large. Because the SiO_4 tetrahedron shows nearly constant bond lengths and a wide variance in bond angles, whereas the TiO_6 octahedron shows nearly ideal bond angles (at least in the range 270°–740°) and a wide variance in bond lengths, we feel that the bond angle variance parameters are not wholly adequate measures of polyhedral distortion for this structure.

Changes in polyhedral volumes over the temperature range 25°C to 740°C are −0.31, 1.52, and 2.05 percent, respectively for the SiO_4 tetrahedron, the TiO_6 octahedron, and the CaO_7 polyhedron. The negligible changes in tetrahedral volume and mean Si–O distance with temperature are consistent with those found in other silicates studied at high temperature. The relative volume and bond length changes among the three polyhedra support the commonly held notion that bond strengths decrease in the series Si^{IV}–O, Ti^{VI}–O, and Ca^{VII}–O.

Nature of the phase transition in titanite and domain formation

The rapid, nonquenchable behavior of the phase transition and the structural data above and below the transition temperature indicate that the phase transition is displacive in nature and can be classified as a distortional transformation following the nomenclature of Buerger (1971). The gradual rate of disappearance of the $\bar{4}01$ reflection and the apparently continuous behavior of the cell volume with temperature are suggestive of a second order phase transition, but our data do not permit choice between first, second, or higher order. It should be noted that space group $P2_1/a$ is a subgroup of $A2/a$, thus fulfill-

TABLE 6. Orientation of thermal ellipsoid axes (°) and RMS displacements (Å) of Ti, Si, and Ca in synthetic titanite at five temperatures

	25°C	165°C	270°C	515°C	740°C
Ca Ellipsoid					
Axis 1 RMS Amplitude	0.090	0.072	0.111	0.130	0.144
Angle with a	82	86	90	90	90
Angle with b	24	138	0	0	0
Angle with c	73	54	90	90	90
Axis 2 RMS Amplitude	0.104	0.137	0.115	0.132	0.156
Angle with a	94	94	100	96	98
Angle with b	67	132	90	90	90
Angle with c	145	130	146	150	149
Axis 3 RMS Amplitude	0.170	0.188	0.208	0.240	0.258
Angle with a	172	174	170	174	172
Angle with b	85	90	90	90	90
Angle with c	60	61	56	60	59
Ti Ellipsoid					
Axis 1 RMS Amplitude	0.075	0.087	0.100	0.109	0.123
Angle with a	74	130	103	107	121
Angle with b	16	57	52	69	71
Angle with c	94	41	38	22	21
Axis 2 RMS Amplitude	0.086	0.102	0.105	0.125	0.140
Angle with a	85	107	107	97	107
Angle with b	89	61	46	25	36
Angle with c	161	130	119	109	111
Axis 3 RMS Amplitude	0.099	0.115	0.137	0.143	0.145
Angle with a	17	45	158	18	36
Angle with b	106	46	112	77	60
Angle with c	109	98	67	101	92
Si Ellipsoid					
Axis 1 RMS Amplitude	0.050	0.036	0.078	0.090	0.092
Angle with a	68	139	124	101	134
Angle with b	149	127	90	90	90
Angle with c	80	56	10	13	20
Axis 2 RMS Amplitude	0.062	0.079	0.093	0.091	0.104
Angle with a	42	94	90	90	90
Angle with b	87	111	180	180	180
Angle with c	156	146	90	90	90
Axis 3 RMS Amplitude	0.094	0.110	0.094	0.112	0.127
Angle with a	56	49	34	11	44
Angle with b	60	136	90	90	90
Angle with c	68	93	80	103	70

ing a necessary but not sufficient condition for second order transitions (Landau and Lifschitz, 1969).

In cooling through the $A2/a \rightarrow P2_1/a$ transition, Ti has a choice of moving in a positive or negative direction along the O(1)–Ti–O(1) bond from the center of symmetry. The direction of movement cannot be random for each octahedron because random displacements would result in Ti occupying the special position (0.5, 0.25, 0.75) on the average, with a large thermal motion component in the axial direction of the octahedron. The random displacement would therefore cause primitive reflections of the type $k + l$ odd to disappear. Because these reflections are clearly present below the transition temperature (Fig. 1), movement of the Ti atoms must be coupled such that a displacement of one Ti in a positive direction causes its neighboring Ti cations in the chain to be displaced in a positive direction. If this linear coupling does not extend throughout the crystal, it must extend far enough to give rise to domains of sufficient size to diffract X rays coherently. This model is similar to that proposed by Comés *et al.* (1970) for tetragonal $BaTiO_3$.

We now examine the crystal chemical factors which might be expected to influence the orientation and shape of these proposed domains. Our view of the domain structure is schematically represented in Figure 4. Notice that where the domain boundary

TABLE 7. Selected interatomic distances (Å) in synthetic titanite at five temperatures

Polyhedron	25°C	165°C	270°C	515°C	740°C
Ti-Octahedron					
Ti-O(1)	1.768(6)**	1.800(9)	1.867(2)	1.876(2)	1.877(2)
Ti-O(1')	1.970(6)	1.942(9)	1.867(2)	1.876(2)	1.877(2)
Ti-O(2A)	2.006(8)	1.991(13)	1.994(3)	1.998(4)	2.006(5)
Ti-O(2B)	1.967(7)	1.990(13)	1.994(3)	1.998(4)	2.006(5)
Ti-O(3A)	1.982(8)	2.005(14)	2.017(4)	2.020(5)	2.021(5)
Ti-O(3B)	2.044(9)	2.026(15)	2.017(4)	2.020(5)	2.021(5)
MEAN	1.956(7)	1.959(12)	1.959(3)	1.965(4)	1.968(4)
Si-Tetrahedron					
Si-O(2A)	1.621(8)	1.625(15)	1.640(4)	1.641(5)	1.639(5)
Si-O(2B)	1.651(8)	1.655(16)	1.640(4)	1.641(5)	1.639(5)
Si-O(3A)	1.655(7)	1.686(12)	1.646(4)	1.642(5)	1.643(5)
Si-O(3B)	1.630(7)	1.606(12)	1.646(4)	1.642(5)	1.643(5)
MEAN	1.639(7)	1.643(14)	1.643(4)	1.642(5)	1.641(5)
Ca-Polyhedron					
Ca-O(1)	2.265(6)	2.277(7)	2.286(5)	2.274(7)	2.275(7)
Ca-O(2A)	2.422(7)	2.448(12)	2.418(4)	2.427(5)	2.432(5)
Ca-O(2B)	2.400(8)	2.390(11)	2.418(4)	2.427(5)	2.432(5)
Ca-O(3A)	2.385(8)	2.383(17)	2.414(3)	2.428(4)	2.437(5)
Ca-O(3A')	2.673(8)	2.683(13)	2.630(3)	2.639(4)	2.641(4)
Ca-O(3B)	2.428(9)	2.450(16)	2.414(3)	2.428(4)	2.437(5)
Ca-O(3B')	2.580(8)	2.585(12)	2.630(3)	2.639(4)	2.641(4)
MEAN	2.450(8)	2.459(13)	2.459(4)	2.466(5)	2.471(5)

**Uncorrected for thermal motion.*

***Numbers in parentheses represent the estimated standard errors ($1\hat{\sigma}$) in the last decimal place quoted.*

cuts across an octahedral chain, both titanium atoms must be displaced toward or away from the O(1) oxygen. We can therefore consider three types of O(1) oxygens: (1) the normal O(1) oxygen with one Ti displaced toward and the other away from the O(1) site; (2) an O(1) oxygen at a domain boundary where both Ti atoms are displaced away from the site; (3) and O(1) oxygen at a domain boundary where both Ti atoms are displaced toward the site. The sum of the Brown and Shannon (1973) bond strengths (ζ) indicate that a type 1 site is charge balanced (ζ = 2.050), a type 2 site is over-saturated with electron density (ζ = 1.718), and a type 3 site is under-saturated with electron density (ζ = 2.398). We feel that, in the absence of other factors, the crystal will react in such a way as to minimize the number of type 2 and type 3 O(1) sites leading to domain boundaries which run parallel to the octahedral chain (the *a* axis). Substitution of an OH group for O at the O(1) site would tend to withdraw electron density from the Ti–O bonds and favor formation of a type 2 site in the low-temperature modification.[2] Similarly, substitution of Al^{+3} or Fe^{+3} for Ti^{+4},

[2] On the basis of Pauling bond strength arguments, Zachariasen (1930) suggested that OH for O substitutions occur at O(1). Utilizing the more recent Brown and Shannon bond strength equations, we find the following bond strength sums to the oxygens at 25°C: ζ[O(1)] = 2.050; ζ[O(2A)] = 1.888; ζ[O(2B)] = 1.873; ζ[O(3A)] = 2.010; ζ[O(3B)] = 2.008 v.u. On the basis of these bond strength sums alone, one might predict that OH should substitute at O(2A) or O(2B). However, an O(1) oxygen at a domain boundary (type 2) is more oversaturated than O(2A) or O(2B), and substitution of OH at this type of O(1) site would lead to a greater charge balancing effect. These arguments are consistent with the earlier suggestion concerning the location of OH in titanite based on polarized infrared data (Isetti and Penco, 1968).

TABLE 8. Selected bond angles (°) of synthetic titanite at five temperatures

Polyhedron	25°C	165°C	270°C	515°C	740°C
Ti-Octahedron					
O(1)-Ti-O(1')	178.9(2)*	179.7(9)	180.0	180.0	180.0
O(1)-Ti-O(2A)	92.8(3)	92.7(5)	90.1(1)	90.2(1)	90.4(1)
O(1')-Ti-O(2A)	86.8(3)	87.6(5)	89.9(1)	89.8(1)	89.6(1)
O(1)-Ti-O(2B)	93.5(3)	92.3(5)	90.1(1)	90.2(1)	90.4(1)
O(1')-Ti-O(2B)	86.9(3)	87.4(5)	89.9(1)	89.8(1)	89.6(1)
O(1)-Ti-O(3A)	91.3(3)	90.4(6)	92.0(2)	92.1(2)	92.0(2)
O(1')-Ti-O(3A)	87.7(4)	89.8(4)	88.0(2)	87.9(2)	88.0(2)
O(1)-Ti-O(3B)	94.5(3)	94.3(5)	92.0(2)	92.1(2)	92.0(2)
O(1')-Ti-O(3B)	84.3(3)	85.6(4)	88.0(2)	87.9(2)	88.0(2)
O(2A)-Ti-O(2B)	173.6(3)	174.9(5)	180.0	180.0	180.0
O(2A)-Ti-O(3A)	90.0(3)	89.9(6)	90.1(2)	90.1(2)	90.1(2)
O(2A)-Ti-O(3B)	88.7(3)	88.7(7)	89.9(2)	89.8(2)	89.9(2)
O(2B)-Ti-O(3A)	91.0(3)	91.2(7)	90.1(2)	90.1(2)	90.1(2)
O(3A)-Ti-O(3B)	174.1(3)	175.2(6)	180.0	180.0	180.0
Si-Tetrahedron					
O(2A)-Si-O(2B)	103.5(3)	103.3(3)	102.9(3)	103.3(3)	103.3(4)
O(2A)-Si-O(3A)	112.4(4)	111.1(7)	112.8(2)	112.7(2)	112.7(2)
O(2A)-Si-O(3B)	107.9(4)	109.5(6)	108.7(2)	108.7(2)	108.7(2)
O(2B)-Si-O(3A)	109.1(4)	108.0(6)	108.7(2)	108.7(2)	108.7(2)
O(2B)-Si-O(3B)	112.9(4)	114.0(8)	112.8(2)	112.8(2)	112.7(2)
O(3A)-Si-O(3B)	111.0(3)	110.6(3)	110.9(3)	110.8(4)	110.5(4)
MEAN	109.5(4)	109.4(6)	109.5(2)	109.5(3)	109.4(3)
Octahedral Chain Kink					
Ti-O(1)-Ti'	141.3(3)	141.6(4)	141.9(3)	141.2(4)	141.3(4)

Numbers in parentheses represent standard errors ($1\hat{\sigma}$) in the last decimal place quoted.

which reduces the positive charge in the vicinity of O(1), will tend to favor the formation of a type 3 site. Thus the presence of impurities may promote formation of domain boundaries which cut across the octahedral chain, effectively reducing the domain size. Experimental evidence supporting this view has been presented by Speer and Gibbs (1974, 1976). It should be emphasized that the substitution of Fe, Al, and OH need not be spatially coupled since the structure at a domain boundary could provide the necessary charge balance.

Comparison with distortional transformations in other compounds

Distortional transformations are known to occur in a number of silicate minerals including quartz, tridymite, cristobalite, nepheline, leucite, albite, anorthite, primitive cummingtonite, pigeonites, $P2_1/c$ clinopyroxenes, and others. In each case cooling through the transition temperature results in a choice of movement of the structural elements involved. Slow cooling through the transition region is thought to favor the growth of large domains, *i.e.*, a coupling of these movements over large volumes of the crystal; whereas fast cooling is thought to favor the growth of small domains, *i.e.*, a coupling of displacements over small regions. Because domain size is also related to composition in most cases, an interpretation of a mineral's cooling history based on domain size is relatively complicated. The coupled displacements of Ti in titanite are somewhat analogous to the coupled tilting of tetrahedra involved with the α–β quartz transition (Young, 1962; Buerger, 1971), although the former involves a change in bond length and the latter a change in bond angle. The proposed domains in titanite resulting from mis-

TABLE 9. Polyhedral distortions (°) and volumes (Å³) of synthetic titanite with increasing temperature (°C).

Polyhedron	25°C	165°C	270°C	515°C	740°C	%Δ*
Ti-Octahedron						
σ^2(oct.)**	8.732	7.044	1.402	1.670	1.557	-82.17
V***	9.988	9.983	10.005	10.092	10.140	1.52
Si-Tetrahedron						
σ^2(tet.)**	12.200	12.896	13.831	12.256	12.165	-0.29
V***	2.264	2.265	2.262	2.257	2.257	-0.31
Ca-Polyhedron						
V***	19.669	19.797	19.733	19.951	20.072	2.05

*% change from 25°C to 740°C.

**Polyhedral distortions were estimated using the formulae for octahedral and tetrahedral bond angle variance of Robinson et al. (1971) and the angles in Table 7.

***Polyhedral volumes were calculated using a modified version of C.T. Prewitt's unpublished program DRLL.

takes in the coupled displacements are analogous to the Dauphine-twin domains in α-quartz. Comparison of the transition mechanism in titanite with that found in pigeonites (Brown *et al.*, 1972), $P2_1/c$ clinopyroxenes (Smyth and Burnham, 1972), and $P2_1m$ cummingtonites (Sueno *et al.*, 1972) illustrates an interesting contrast. Whereas these chain silicates transform from high to low temperature forms by a kinking of the chains of tetrahedra and concomitant changes in the adjacent octahedral sites, the high to low transformation in titanite involves essentially no change in the kink angles of the chains of corner-sharing Ti-octahedra (Table 7). This difference in mechanism can be rationalized in terms of the fact that isolated silicate tetrahedra in titanite rigidly link adjacent octahedra in a given octahedral chain, preventing significant unkinking or kinking above or below the transition. On the other hand, the adjacent silicate tetrahedra within the chains in primitive clinopyroxenes and clinoamphiboles are weakly linked by octahedral cations. Thus changes in the kink angle of these tetrahedral chains are more energetically favored with changes in temperatures.

Because of the antiparallel array of Ti displacements between adjacent octahedral chains, it has been suggested that titanite is an antiferroelectric (Speer and Gibbs, 1974). We note here some further similarities between the transition in titanite and the ferro- or antiferroelectric to paraelectric transition in some perovskite structure compounds. For example, $BaTiO_3$ loses its net dipole moment at 120°C when it undergoes a transition from tetragonal to cubic. This transition is associated with a shift in Ti from an off-center position to the geometric center of the TiO_6 octahedron, similar to that observed in titanite. The shift is 0.12 Å in $BaTiO_3$ compared with 0.10 Å in titanite. Both $BaTiO_3$ and titanite show a shortening of the cell direction which is parallel to the Ti displacements, though the magnitude of change is smaller in titanite than in $BaTiO_3$ (Kay and Vousden, 1949). Because the silicate tetrahedra tend to hold the octahedral chain rigid in titanite, there is little or no tilting of the octahedra at the transition, as is found in some perovskites. Titanite would therefore correspond to those perovskites which show a purely displacive change (*e.g.*, $BaTiO_3$) rather than tilting (*e.g.*, $SrTiO_3$) or a combination of displacement and tilting (*e.g.*, $NaNbO_3$) (Megaw, 1973). These observations are only qualitative, and measurements of the dielectric constant of titanite as a function of temperature are needed to demonstrate that titanite undergoes an antiferroelectric to paraelectric transition.

Conclusions

In conclusion we have shown that titanite undergoes a fast, nonquenchable phase transition from space group $P2_1/a$ at 220° ± 20°C primarily in-

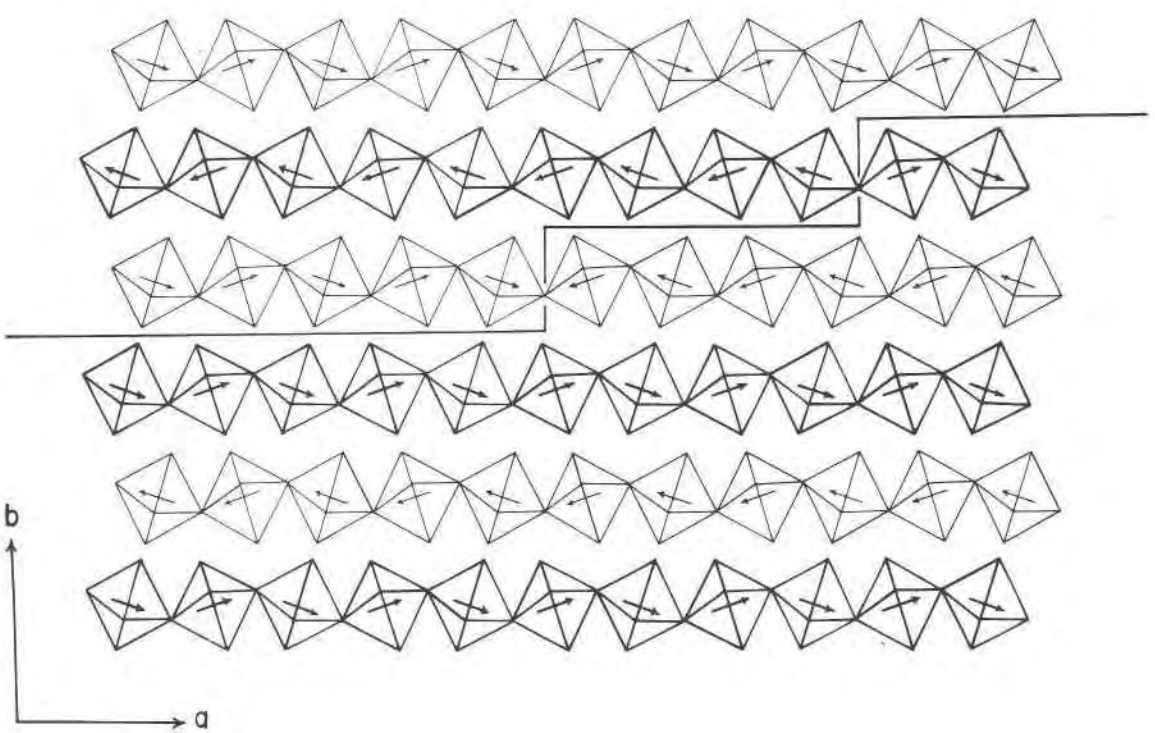

FIG. 4. Domain model of titanite showing the chains of Ti-octahedra parallel to *a*. The chains with dark and light outlines represent those above and below the plane of the drawing. Arrows represent directions of displacement of the Ti-cations. The regions on either side of the heavy line through the figure represent domains in opposite orientations. Two types of O(1) sites are located at the vertical domain boundaries: that with both Ti-cations displaced away from O(1) (upper right) and that with both displaced towards O(1) (center).

volving the movement of the Ti atom from an off-center position to the geometric center of the TiO_6 octahedron. Whether this involves a true movement or a disorder between two sites related by a center of symmetry cannot be deduced from our crystallographic data; however, we favor the former interpretation. Our data are consistent with a second order phase transition. As in $BaTiO_3$, synthetic titanite shows a shortening of the cell in the direction parallel to the Ti displacement in the temperature region of the transition. The transition mechanism permits the formation of domains related by a two-fold axis parallel to *b* as suggested by Speer and Gibbs (1974); domain size is probably controlled by impurity content and distribution as well as by cooling rate. The substitution of OH for O and of Fe and Al for Ti at or adjacent to O(1) sites at domain boundaries appears to be especially important in this respect. A study of the effect of controlled amounts of impurities on the $k + l$ odd reflections is called for. The similarity between the structural changes in titanite and those in $BaTiO_3$ suggest that titanite might show antiferroelectric behavior.

Acknowledgments

We wish to thank Professor G. V. Gibbs (Virginia Polytechnic Institute and State University) for providing the crystals of synthetic sphene used in this study and for making details of his room-temperature refinement available to us prior to publication. Our study was supported by grants from the Stanford Research Development Fund and the National Science Foundation (NSF GA 41731). We gratefully acknowledge Standard Oil of California for providing computer time for this project.

References

BROWN, G. E., C. T. PREWITT, J. J. PAPIKE AND S. SUENO (1972) A comparison of the structures of low and high pigeonite. *J. Geophys. Res.* **77**, 5778–5789.

BROWN, G. E., S. SUENO AND C. T. PREWITT (1973) A new single-crystal heater for the precession camera and four-circle diffractometer. *Am. Mineral.* **58**, 698–704.

BROWN, I. D. AND R. D. SHANNON (1973) Empirical bond-strength–bond-length curves for oxides. *Acta Crystallogr.* **A29**, 266–282.

BUERGER, M. J. (1971) Crystal-structure aspects of phase transformations. *Trans. Am. Crystallogr. Assoc.* **7**, 1–23.

COMÉS, R., M. LAMBERT AND A. GUINIER (1970) Désordre linéaire dans les cristaux (cas du silicium, du quartz et des perovskites ferroelectriques). *Acta Crystallogr.* **A26**, 244–254.

CORFIELD, R., R. J. DOEDENS AND J. A. IBERS (1967) The crystal and molecular structure of nitridodichlorobis (Triphenylphos-

phine) Rhenium (V), $ReNCl_2$ $(P(C_6H_5)_3)_2$, *Inorg. Chem.* **6,** 197–204.

HAMILTON, W. C. (1959) On the isotropic temperature factor equivalent to a given anisotropic temperature factor. *Acta Crystallogr.* **12,** 609–610.

ISETTI, G. AND A. M. PENCO (1968) La posizione dell'Idrogeno ossidrilico nella titanite. *Mineral. Petrogr. Acta,* **14,** 115–122.

KAY, H. F. AND P. VOUSDEN (1949) Symmetry changes in barium titanite at low temperatures and their relation to its ferroelectric properties. *Phil. Mag.* **40,** 1010–1040.

LANDAU, L. D. AND E. M. LIFSCHITZ (1969) *Statistical Physics,* Addison-Wesley Company, Reading, Massachusetts, 484 p.

MEGAW, H. D. (1973) *Crystal Structures: A Working Approach,* W. B. Saunders, Philadelphia, 563 p.

MONGIORE, R. AND L. RIVA DI SANSEVERINO (1968) A reconsideration of the structure of titanite, $CaTiOSiO_4$. *Mineral. Petrogr. Acta,* **14,** 123–141.

MOORE, P. B. (1970) Structural hierarchies among corner-sharing octahedral and tetrahedral chains. *Neues Jahrb. Mineral. Monatsh.* 163–173.

MULLER, O. AND R. ROY (1974) *The Major Ternary Structural Families.* Springer-Verlag, New York, 487 p.

ROBBINS, C. R. (1968) Synthetic $CaTiSiO_5$ and its germanium analogue ($CaTiGeO_5$). *Mater. Res. Bull.* **3,** 693–698.

ROBINSON, K., G. V. GIBBS AND P. H. RIBBE (1971) Quadratic elongation: A quantitative measure of distortion in coordination polyhedra. *Science,* **172,** 567–570.

SMYTH, J. R. AND C. W. BURNHAM (1972) The crystal structures of high and low clinohypersthene. *Earth Planet. Sci. Lett.* **14,** 183–189.

SPEER, J. A. AND G. V. GIBBS (1974) The crystal structure of synthetic titanite, $CaTiOSiO_4$, and the domain texture of natural titanites. *EØS, Trans. Am. Geophys. Union,* **55,** 462.

——— AND ——— (1976) The crystal structure of synthetic titanite, $CaTiOSiO_4$, and the domain textures of natural titanites. *Am. Mineral.* **61,** 238–247.

SUENO, S., J. J. PAPIKE, C. T. PREWITT AND G. E. BROWN (1972) Crystal structure of high cummingtonite. *J. Geophys. Res.* **77,** 5767–5777.

TAYLOR, M. P. AND G. E. BROWN (1974) High-temperature crystal chemistry of sphene. *EØS, Trans. Am. Geophys. Union,* **56,** 1201.

YOUNG, R. A. (1962) Mechanism of the phase transition in quartz. Report 2569, *Air Force Office Scientific Research,* Washington, D.C.

ZACHARIASEN, W. H. (1930) The crystal structure of titanite. *Z. Kristallogr.* **73,** 7–16.

Manuscript received, August 29, 1975; accepted for publication, February 25, 1976.